

# Evaluation of the specific interfacial contact resistance for Al /p-Si contact

H. Amer<sup>a</sup>, H. Tork<sup>a</sup>, A.K. Aboul Seoud<sup>b</sup>, and M. Rizk<sup>b</sup>

<sup>a</sup> Institute of Graduate Studies and Research , Alexandria University, Alexandria, Egypt

<sup>b</sup> Electrical Eng., Dept., Faculty of Eng., Alexandria University, Alexandria, Egypt

The specific interfacial resistance refers to the metal-semiconductor interface. It is a very useful term for ohmic contacts because it is independent of the contact area. In this work, the effect of the different sintering temperatures and sintering times for the Al /p-Si, specific contact resistance have been accurately determined. The data was carried out by a computer program using an interfacing system technique between a specially designed oven furnace and the computer. The specific contact resistance has been determined using the three point probe method. The specific contact resistance decreases from  $0.8 \cdot 10^{-6}$  ohm -cm<sup>2</sup> to  $0.01 \cdot 10^{-6}$  ohm -cm<sup>2</sup> for an increase in the sintering temperature from 573 K to 823 K. The sintering time has no effect on the specific contact resistance. It is hoped that this study can be used in the future as a guideline in developing ohmic contacts for various semiconductor devices.

إن المقاومة النوعية هي مقاومة الطبقة المتداخلة بين شبه الموصل والمعدن. إنها عنصر هام جداً لحساب مقاومة الوصلة، وحيث أنها لا تعتمد على مساحة الوصلة فإنها عامل ملائم عند مقارنة الوصلات ذات المساحات المختلفة. في هذا البحث تم تحديد بكفاءة تأثير المعالجة الحرارية عند درجات الحرارة المختلفة وزمن هذه المعالجة على المقاومة النوعية. تم الحصول على هذه النتائج عن طريق برنامج على الحاسب الآلي متصل بفرن صمم خصيصاً لهذا الغرض - تم حساب المقاومة النوعية عن طريق حساب الثلاث وصلات. وقد وجد أن المقاومة النوعية تقل من  $1.0 \times 10^{-6}$  أوم.سم<sup>2</sup> إلى  $1.0 \times 10^{-7}$  أوم.سم<sup>2</sup> عندما رفعت درجة المعالجة الحرارية من 573 كلفن إلى 823 كلفن، كما وجد أن زمن المعالجة الحرارية ليس له تأثير على المقاومة النوعية للوصلة. نأمل أن تكون هذه الدراسة نواة عند دراسة وصلات لبنائض شبه موصلة.

**Keywords:** Ohmic contact, Characterization, Conduction mechanism

## 1. Introduction

Metallization contact systems are a fundamental component to all semiconductor devices and integrated circuits. They provide the correct electrical link between the active region of the semiconductor and the external circuit. In the case of an integrated circuit, they interconnect with great precision the circuit elements to provide the desired conducting paths. The primary concern in the choice of a metallization contact is to ensure that the metal has the desired electrical properties.

Two distinct contacts can be realized at the metal-semiconductor contact. These are the ohmic (resistive) and the Schottky (rectifying) contacts.

Previous work on Al/p-Si contact used to sinter the contacts before the measurements were taken. In the present work, the

measurements of the current and voltage were taken during the heat-treatment, and so the effect of the sintering temperatures and sintering times are studied more precisely in order to obtain a low resistance ohmic contact. In spite of the fact that the effects of heat treatment has to be considered at the normal operating temperature (room temperature), the measurements in this paper have been taken at the annealing temperature; This may be used to investigate the evolution of the specific contact resistance during heat treatment only.

## 2. Theoretical approach

The only independent parameter that describes the resistance of the interface at the contact is called the specific contact resistivity. It's unit is ohm-cm<sup>2</sup> i.e. it is the resistance of a unit area of the thin interfacial layer between the bulk metal and the semiconductor

substrate. A theoretical definition for the specific contact resistance is

$$\rho_c = dV/dJ \quad \left| \quad J=0, \right. \quad (1)$$

where J is the current density and V is the voltage drop across the interface.

The implicit assumption underlying eq. (1) is that J is uniform across the contact interface. Eq. (1) is applied to contacts that over specified range of currents are ohmic.

### 2.1. Effect of heat treatment

Most contacts used in semiconductor devices are subjected to heat treatment. This may be deliberately to promote adhesion of the metal to the semiconductor or they are unavoidable because a high temperature is needed for other processing stages to occur after the metal is deposited.

### 2.2. The Al-Si system

During sintering, Si from the single crystal substrate diffuses into the Al through the grain boundaries, this is called solubility, concomitantly, Al diffuses to the substrate surface, this is called penetration. The extent of the penetration is greater for higher temperatures because diffusion rates are higher and there is a higher solubility of Si in Al.

Since the solubility of Si in Al decreases with decreasing temperature, Al becomes supersaturated with Si during cooling from the sintering temperature. The supersaturation is highest in the region adjacent to the contact from which Si was originally depleted. During cooling the Si precipitates from the solution in the Al forming particles at the Al boundaries, and at the same time forming an epitaxial layer on the Si in the contact region. So the effective density of the dopant in the semiconductor; is increased, the barrier gets thinner (the depletion width gets smaller) and thermionic or even field emission occurs. A p<sup>+</sup>-p system is formed.

The calculation of  $\rho_c$  has been derived from different approaches [1-5]. Unfortunately, the published curves do not emphasize the

practical regimes used for Si contacts and more detailed curves are needed.

Furthermore, those results did not consider in details the relevant tunneling effective masses, and the respective effective dielectric constant that results in n and p-type materials under the effect of temperature. In this study the calculation of the effective masses of carriers and relative dielectric constants have been taken into consideration.

### 2.3. The current transport

The value of  $\rho_c$  is determined for Field Emission (FE), Thermionic Emission (TE) and Thermionic Field Emission (TFE) transports. The most widely accepted model for FE and TFE is given by Padovani and Stratton [6-7] and is used in this work. Yu [4] has utilized his theory to calculate  $\rho_c$ , he used a useful term  $E_{00}$  (a parameter which plays an important role in tunneling theory. It has the dimensions of energy divided by charge ) and is defined as

$$E_{00} = (q\hbar/2) \sqrt{N/m^*_{tun} \epsilon_s}, \quad (2)$$

where  $m^*_{tun}$  is the tunneling effective mass of electrons or holes in the semiconductor, N is the doping concentration,  $\epsilon_s$  is the permittivity of the semiconductor, q is the electronic charge and  $\hbar$  is the modified Plank's constant. For any particular ellipsoid of constant energy surface in K space, the  $m^*_{tun}$  is given by [8]

$$m^*_{tun} = \left( \frac{l^2}{m_x} + \frac{m^2}{m_y} + \frac{n^2}{m_z} \right)^{-1}, \quad (3)$$

where l, m and n are the direction cosines of the ellipsoid relative to the principle axes, and  $m_x$ ,  $m_y$ , and  $m_z$  are the tensor masses. The dominant current conduction mechanism and thus  $\rho_c$  can be divided into three regions.

In the low doping region  $kT/E_{00} \gg 1$ , TE dominates and

$$\rho_c = (k/qA^{**}T) \exp(\phi_b/kT). \quad (4)$$

Where  $A^{**}$  is the modified Richardson constant [9] and  $\phi_b$  is the barrier height.

In the medium doping region  $kT/E_{00} \approx 1$ , FE

dominates and,

$$\rho_c = \frac{k\sqrt{E_{00}}}{qA^{**}T\sqrt{\pi(\phi_b + u_f)}} \cosh\left(\frac{E_{00}}{kT}\right) \coth\left(\frac{E_{00}}{kT}\right) \cdot \exp\left(\frac{\phi_b + u_f}{E_0} - \frac{u_f}{kT}\right), \quad (5)$$

where  $u_f$  is the Fermi level with respect to the band edge (positive when generate),  $T$  is the absolute temperature,  $k$  is the Boltzmann constant and  $A^*$  is the effective Richardson constant and is equal to

$$A^* = M 4 \pi m^* q k^2 / h^3, \quad (6)$$

and

$$E_0 = E_{00} \coth(E_{00} / kT). \quad (7)$$

$E_0$  is a measure of the tunneling probability in TFE and TE,  $M$  is the number of equivalent ellipsoids corresponding to the minimum tunneling effective mass and  $m^*$  is the effective mass of electrons and holes and is different from  $m^*_{\text{tun}}$  and is given by[10]

$$m^* = (l^2 m_y m_z + m^2 m_x m_z + n^2 m_x m_y)^{1/2}.$$

Eq. (4) is valid if;

$$\frac{\cosh^2\left(\frac{E_{00}}{kT}\right)}{\sinh^3\left(\frac{E_{00}}{kT}\right)} < \frac{2(\phi_b + u_f)}{3E_{00}}, \quad (8)$$

for higher doping,  $kT / E_{00} \ll 1$ , TFE dominates and

$$\rho_c = \left( \frac{A^* q T \pi}{k \sin(\rho c k T)} \exp\left(\frac{-\phi_b}{E_{00}}\right) - \frac{A^* q}{c k^2} \exp\left(\frac{-\phi_b}{E_{00}} - c u_f\right) \right)^{-1}, \quad (9)$$

where ;

$$c = \frac{1}{2 E_{00}} \ln\left(\frac{4 \phi_b}{u_f}\right). \quad (10)$$

### 3. Experimental procedure

The p-type Si[100] crystals used in these experiments are doped with boron of doping concentration  $N_A = 10^{24} \text{ m}^{-3}$ . Prior to metal deposition the samples were degreased by immersing them successively in propanol and HF 40%, they are then dried by using a filter paper. A thick layer of Al was evaporated on the polished surface of the sample in the vacuum chamber Edward E 306A. Circular dots of .5 mm in diameter were obtained by using a special mask .The measured specific contact resistance at room temperature was  $5 \cdot 10^{-6} \text{ ohm-cm}^2$

### 4. Results and discussion

The I-V characteristics of the metal semiconductor junction are drawn using the Grapher program at six different temperatures 573K, 623K, 673K, 723K, 773K and 823K. Figs. 1 to 6 show these I-V characteristics at the different sintering times. The readings of the currents and voltages were obtained using the three point probe method [11]. The specific contact resistance  $\rho_c$  are obtained from the slope of the best fitting lines to the I-V characteristics.

Fig.7 shows the effect of the sintering temperatures on  $\rho_c$ , the decrease in  $\rho_c$  with the increase of the temperature is due to the increase of the doping concentration just under the metal contact. Fig. 8 shows the relation between  $\rho_c$  and the sintering time, the increase of the sintering time has no effect on the specific contact resistance  $\rho_c$  because the contact has reached its thermal stability.

The evaluation of  $N_A$  was obtained from the solid solubility of Al in Si [12]. The values of  $N_A$  at the different temperatures are reported in table 1.

The theoretical dependence of the specific contact resistance  $\rho_c$  on the doping concentration was published by Piotrowska [13].

Table 1  
Values of  $N_A$  at different temperatures

| T (K)     | 300       | 573                | 623                | 673       | 723                  | 773                | 823                  |
|-----------|-----------|--------------------|--------------------|-----------|----------------------|--------------------|----------------------|
| $N_A/m^3$ | $10^{24}$ | $5 \times 10^{25}$ | $9 \times 10^{25}$ | $10^{26}$ | $1.5 \times 10^{26}$ | $2 \times 10^{26}$ | $2.5 \times 10^{26}$ |

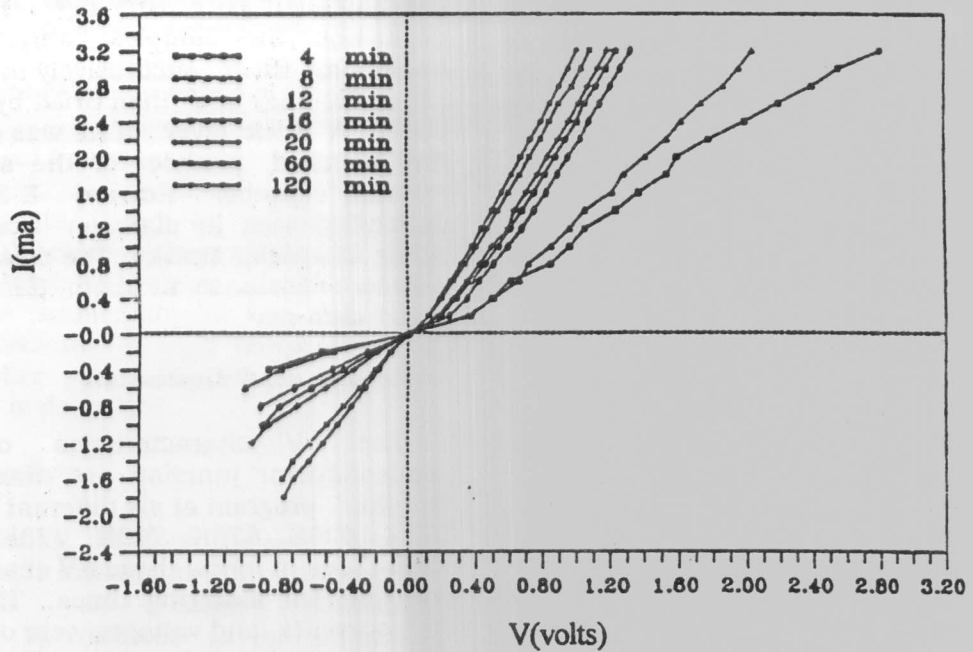


Fig. 1. The I-V characteristics at 537K and different sintering times.

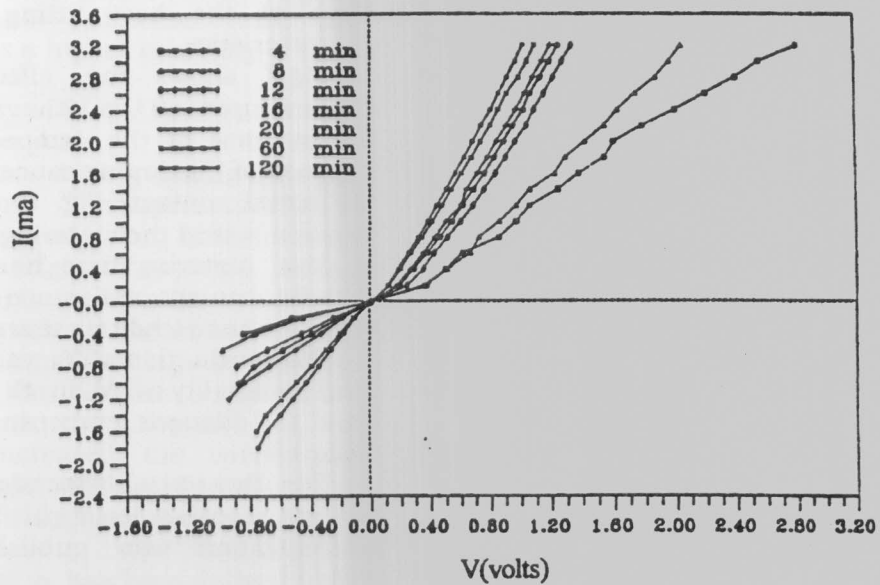


Fig. 2. The I-V characteristics at 623K and different sintering times.

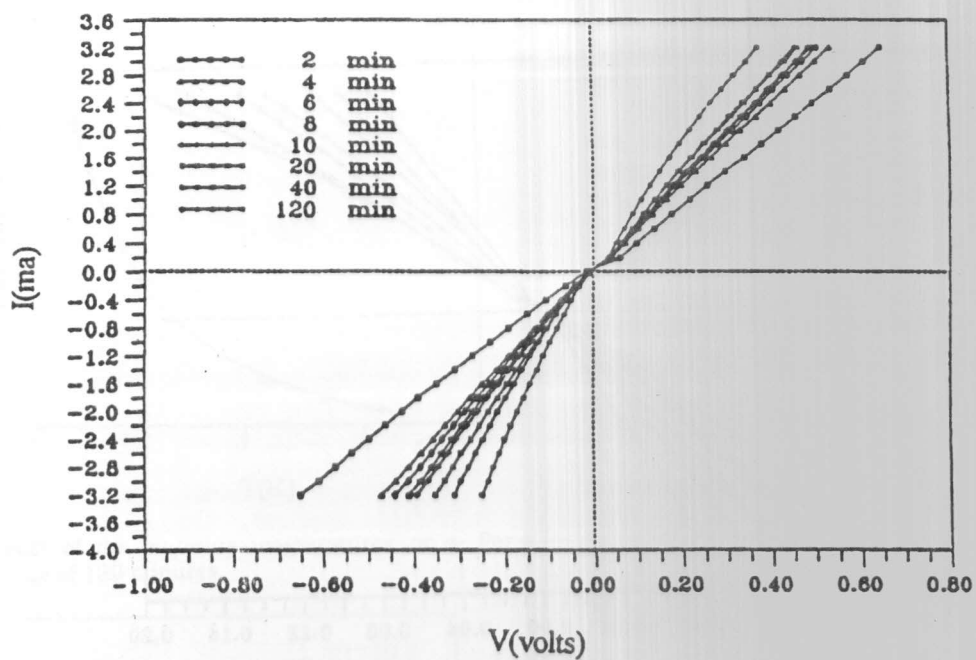


Fig. 3. The I-V characteristics at 673K and different sintering times.

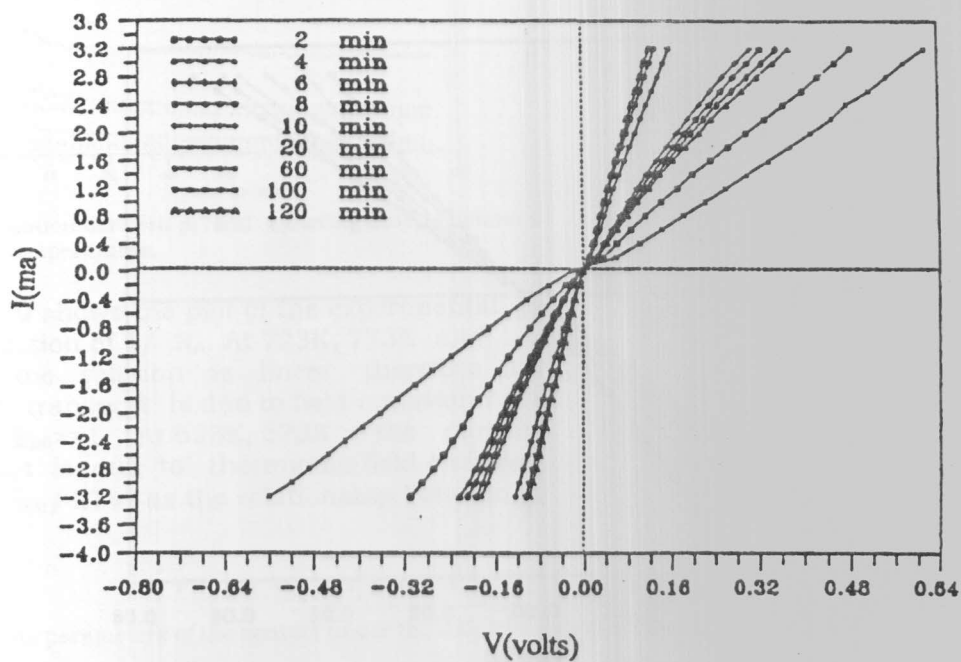


Fig. 4. The I-V characteristics at 723 and different sintering times.



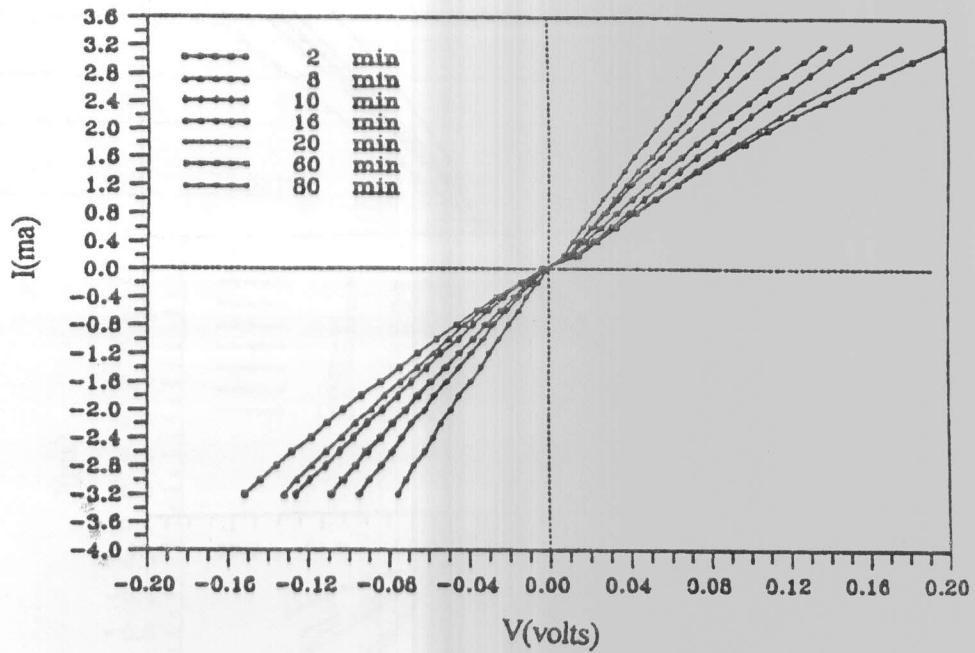


Fig. 5. The I-V characteristics at 773K and different sintering times.

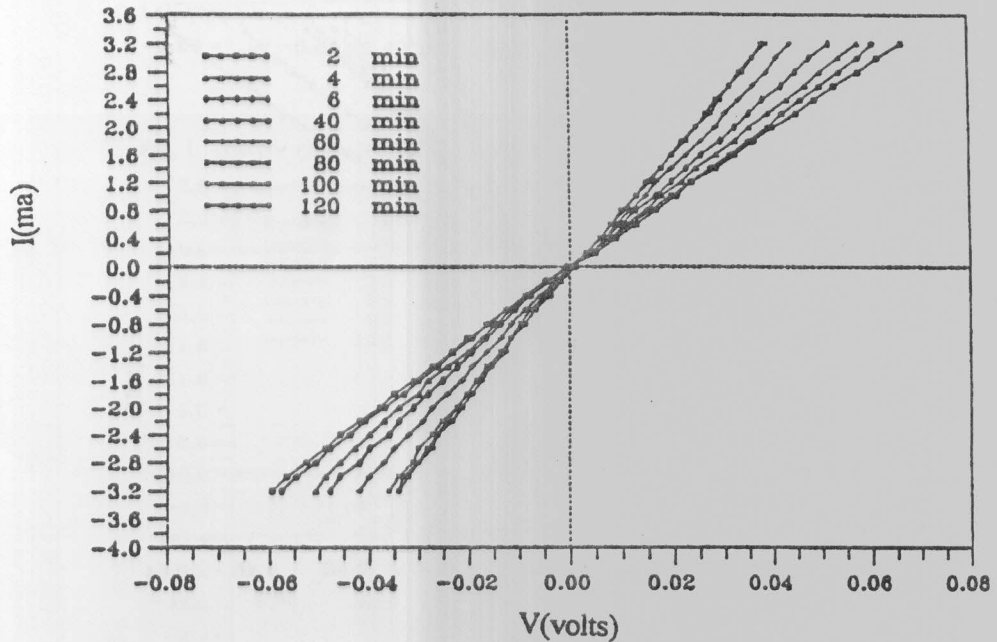


Fig. 6. The I-V characteristics at 823K and different sintering times.

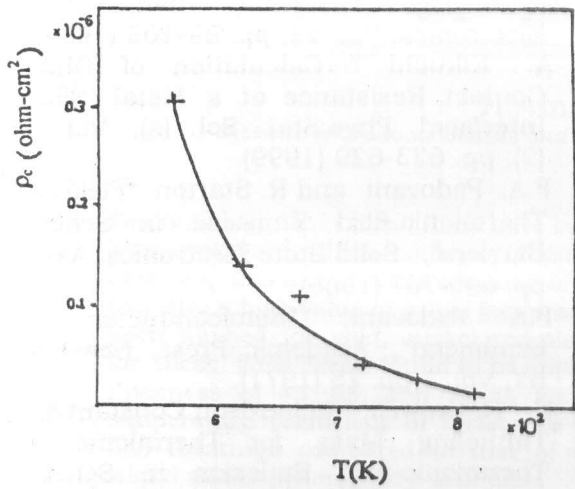


Fig. 7. Effect of the sintering temperatures on  $\rho_c$ . For a sintering time of 120 minutes.

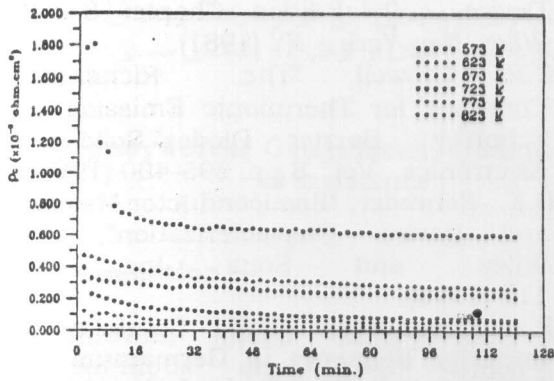


Fig. 8. Relation between  $\rho_c$  and sintering time at different sintering temperatures.

Fig. 9 shows the plot of the experimental  $\rho_c$  as a function of  $1/\sqrt{N_A}$ . At 723K, 773K and 823K, the relation is linear therefore the current transport is due to field-emission with  $kT / E_{00} \gg 1$ . At 623K, 673K the current transport is due to thermionic-field emission with  $E_{00}/ kT \approx 1$  as the relationship between  $\rho_c$

and  $1/\sqrt{N_A}$  deviates from linearity. At 573K the current transport is due to thermionic emission with  $kT / E_{00} \gg 1$ .

Table 2 shows the various parameters of the contact under the different experimental temperatures. The effective tunneling mass  $m^*_{tun}$  has been calculated according to [14]. The dielectric constant  $\epsilon_s$  has been calculated according to [15]. The different  $E_{00}$  values are in agreement with the different type of the conduction mechanisms obtained in Fig. 9. Taking  $A^{**}=32 \text{ A/cm}^2/\text{K}^2$  for p-silicon, the barrier height in the thermionic emission was found to be equal to .36 eV as determined from eq. (4). In the field emission region,  $\rho_c$  depends linearly on  $1/\sqrt{N_A}$  with a slope equal to  $[2\sqrt{m^*_{tun}\epsilon} / qh] \phi_b$ . Table 3 shows the values of  $\phi_b$  in the field-emission region. Fig. 10 shows the effect of the sintering temperature on the barrier height  $\phi_b$ .

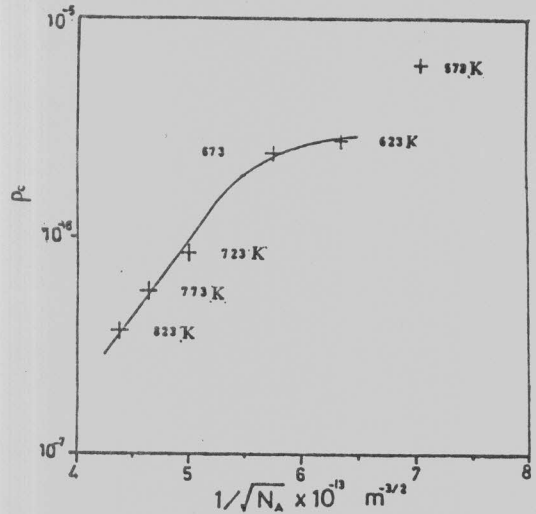


Fig. 9. Experimental relation between  $\rho_c$  and  $1/\sqrt{N_A}$ .

Table 2  
The various parameters of the contact under the different experimental temperatures

| T (K)                               | 300       | 573                | 623                | 673       | 723                  | 773                | 823                  |
|-------------------------------------|-----------|--------------------|--------------------|-----------|----------------------|--------------------|----------------------|
| $KT/q \times 10^{-2}$               | 2.58      | 4.94               | 5.37               | 5.8       | 6.235                | 6.66               | 7.09                 |
| $m^*_{tun}$                         | .8        | .9                 | .92                | .95       | .97                  | 1                  | 1.2                  |
| $\epsilon_s$                        | 11.7      | 12                 | 12.5               | 12.8      | 13                   | 13.5               | 13.8                 |
| $N_A (\text{m}^{-3})$               | $10^{24}$ | $5 \times 10^{25}$ | $9 \times 10^{25}$ | $10^{26}$ | $1.5 \times 10^{26}$ | $2 \times 10^{26}$ | $2.5 \times 10^{26}$ |
| $E_{00} \times 10^{-2} (\text{eV})$ | .6        | 4                  | 5.37               | 5.8       | 6.4                  | 7.1                | 7.22                 |
| $m^*_{tun}\epsilon_s$               | 9.36      | 10.8               | 11.5               | 12.1      | 12.6                 | 13.5               | 16.36                |
| $\rho_c \times 10^{-6} (\Omega)$    | .84       | .6                 | .38                | .3        | .15                  | .08                | .02                  |

Table 3  
Values of  $\phi_B$  in the field-emission region  
at the different temperatures

| T (K)         | 723  | 773   | 823   |
|---------------|------|-------|-------|
| $\phi_b$ (eV) | 0.19 | 0.102 | 0.096 |

## 5. Conclusions

When this work was carried out we were faced with the fact of definitive measurements of both barrier height and surface doping concentration. A survey on the reported values of the specific resistance shows that its values varies substantially from one report to the other. A problem has been raised. Why? . What are the main factors which affect these values?. In the calculation of the doping concentration it is very difficult to accurately measure the electrical active concentration at the surface, even values taken by the SIMS are often overestimated since not all chemical doping is activated. But by using the proposed interface system, the effect of the different sintering temperatures and sintering times for the Al/P-Si specific contact resistance have been measured at the annealing temperatures. The specific contact resistance decreases from  $0.8 \cdot 10^{-6}$  ohm-  $\text{cm}^2$  to  $0.01 \cdot 10^{-6}$  ohm-  $\text{cm}^2$  for an increase in the sintering temperature from 573 K to 823 K. The sintering time has no effect on the specific contact resistance.

It is hoped that this study can be used in the future as a guideline in developing ohmic contracts for various semiconductor devices

## References

- [1] C. Y. Chang, Y.K. Fang and S.M. Sze, "Specific Contact Resistance of Metal-Semiconductor Barriers", *Solid State Electronics*, Vol. 14, pp. 541-550 (1971).
- [2] M.P. Lepselter and J.M. Andrews, "Ohmic Contacts to Silicon" in *Ohmic Contacts to Semiconductors*. B Schwartz, Ed. New York, NY: Electrochem. Soc., pp. 159-161 (1969).
- [3] A.Y.C.Yu "Electron Tunneling and Contact Resistance of Metal-Silicon Contact Barriers", *Solid State Electronics*, Vol. 13, pp. 239-247 (1970).
- [4] C.R. Crowell and V.L. Rideout, "Normalized Thermionic-Field (T-F) Emission in Metal-Semiconductor

- (Schottky) Barriers", *Solid State Electronics*, Vol. 12, pp. 89-105 (1969).
- [5] A. Kikuchi " Calculation of Ohmic Contact Resistance at a Metal /Silicon Interface". *Phys.Stat. Sol. (a)*, Vol. 175 (2), pp. 623-629 (1999).
- [6] F.A. Padovani and R. Starton. "Field and Thermionic-field Emission in Schottky Barriers", *Solid State Electronics.*, Vol. 9, pp. 695-707 (1966).
- [7] F.A Padovani, "Semiconductor and Semimetal", Academic Press, New-York, NY, Vol. 7 pp. 75 (1971).
- [8] C. R. Crowell, "Richardson Constant and Tunneling Mass for Thermionic and Thermionic-field Emission in Schottky Barrier Diodes", *Solid State Electronics*, Vol. 12, pp. 55-58 (1969).
- [9] S.M. Sze, *Physics of Semiconductor Devices*,. 2<sup>nd</sup> Edition. Chapter 8. John Wiley, New York , NY (1981).
- [10] C.R. Crowell, "The Richardson Constant for Thermionic Emission in Schottky Barrier Diodes", *Solid-state Electronics*, Vol. 8 pp. 395-400 (1965).
- [11] D.K. Schroder, "Semiconductor Material and Device Characterization", John Wiley and Sons Inc., pp. 110 (1990).
- [12] F.A. Trumbore, "Solid Solubility of Impurity Elements in Germanium and Silicon.", *Bell. Syst. Tech. J.*, Vol. 39, pp. 205-207 (1960).
- [13] Piotrowska, H.A. Guivarc' and G. Pelous "Ohmic Contact to III-V Compound Semiconductors: A review of Fabrication Techniques." *Solid-state Electronics*, Vol. 26 (3), pp. 179-197 (1983).
- [14] R. Vankemmel W. Schoenmaker and K.De. Meyer "A Unified Temperature Range Model for The Energy Gap, the Effective Carrier Mass and Intrinsic Concentration in Silicon.", *Solid-state Electronics*, Vol. 36 (10), pp. 1379-1384 (1993).
- [15] P. Dautenschlager, M. Garriga, L. Vina and M. Cardona "Temperature Dependence of the Dielectric Function and Inter-band Critical Points in Silicon." *Phys. Rev. B*, Vol. 36 (3), pp. 4821- 4830 (1987).

Received: February 20, 2000  
Accepted: July 31, 2001